

# Enhancing cryogenic thermal diode performance via temperature-dependent contact resistance

Katja Vozel<sup>1</sup>, Darja Gačnik<sup>1</sup>, Andrej Kitanovski<sup>1</sup>

<sup>1</sup>Faculty of Mechanical Engineering, University of Ljubljana, Askerceva 6, 1000 Ljubljana, Slovenia

In macroscopic solid-state thermal diodes (MSTDs), spatial and temperature asymmetry arises from combining two materials whose thermal conductivities vary differently with temperature<sup>[1]</sup>. These devices offer strong potential for passive directional heat control in cryogenic environments. However, current state-of-the-art MSTDs exhibit rectification factors (RF) that remain too low for practical implementation. The RF is defined as the ratio between forward and reverse heat flux,  $\dot{q}_{\text{forward}}/\dot{q}_{\text{reverse}} - 1$ . Examples of approaches to improving performance include introducing asymmetries via nanoscale defects<sup>[2]</sup> and examining the effects of thermal contact resistance (TCR)<sup>[3]</sup>.

Our analysis explores a new approach to enhance MSTD performance: leveraging the temperature dependence of TCR. At cryogenic temperatures, TCR increases exponentially with decreasing temperature due to a transition from diffusive to ballistic heat transport<sup>[4]</sup>. This occurs when the mean free path of heat carriers approaches the characteristic surface roughness of the contact interface. This effect, combined with suitable material thermal conductivities, can further enhance asymmetric heat flow across the interface.

We investigate this numerically using Fourier's law and the finite volume method. The temperature dependence of the materials' thermal conductivities and the TCR are incorporated into the model. Thermal expansion is neglected. Examples of temperature-dependent TCR values at low temperatures as well as thermal conductivities are taken from the literature<sup>[5,6]</sup> and shown in Figure 1. The material pairs considered are: rhodium-iron alloy (RhFe) - sapphire ( $\text{Al}_2\text{O}_3$ ), and diamond (C) - gold (Au). Rh thermal conductivity is used as a proxy for RhFe due to the missing available data.

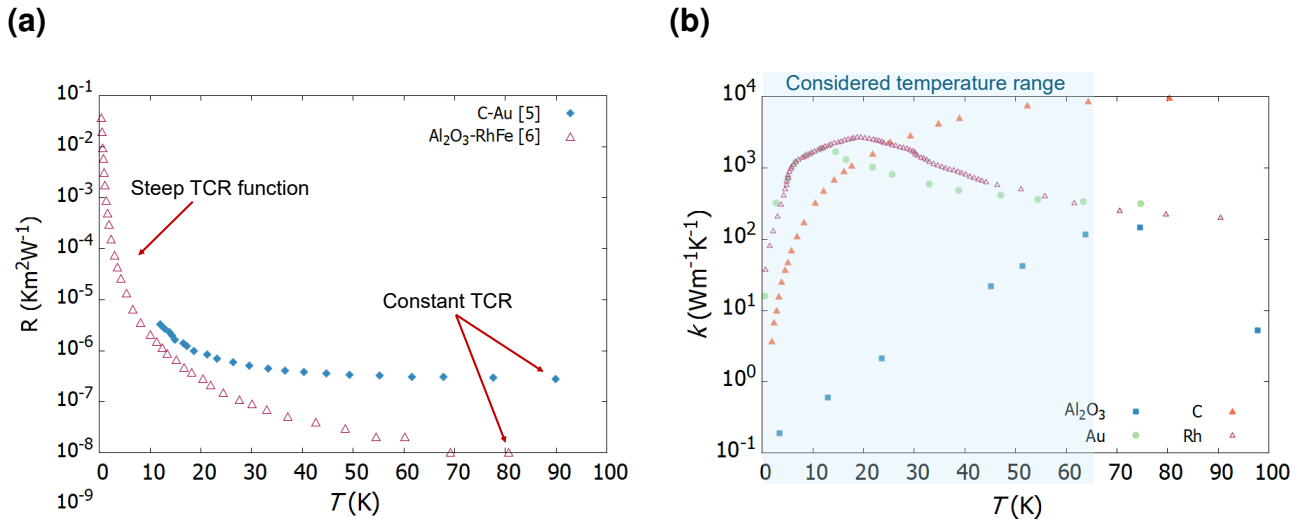


**Figure 1.** Thermal contact resistance for pairs of known materials and their thermal conductivities at low temperatures. **(a)** TCR value between different materials. The values of the TCR are theoretically determined values from the reference papers<sup>[5,6]</sup>. **(b)** Thermal conductivity of selected materials at low temperatures.

The MSTDs in this study are modeled with segments of equal length  $L = 100 \mu\text{m}$  (Figure 2) and fixed terminal temperatures. Cold terminal temperature  $T_{\text{cold ter.}}$  is set for each material pair individually, between just above 0 and 20 K. The thermal bias  $\Delta T = T_{\text{hot ter.}} - T_{\text{cold ter.}}$  ranges from 5 to 45 K. Forward and reverse biases are realized by swapping the terminal temperatures.

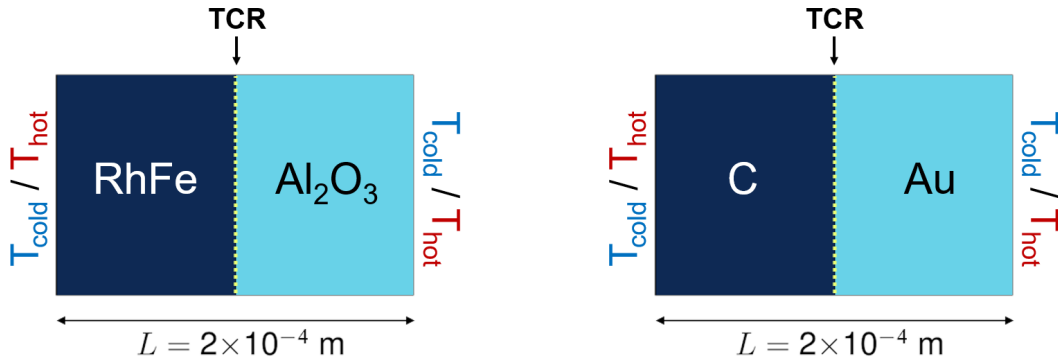


**Figure 2.** Representative MSTD configurations used in the analysis of the impact of temperature-dependent TCR at material interfaces on device performance.

The calculated RF values are compared with the case where the TCR is not temperature-dependent and has a constant value equal to the value above 100 K (Figure 1a). This com-

parison isolates the temperature dependence of the TCR to assess its influence relative to the TCR itself.

Figure 3 shows the simulation results across different temperature intervals. The results reveal a substantial increase in RF in some cases, particularly when the MSTD operates in the temperature range where the TCR function is steepest. The most significant improvement in the RF value occurs for material pair RhFe -  $\text{Al}_2\text{O}_3$  (Figure 3a), when the RF increases from  $6 \times 10^{-3}$  (in the case of a constant TCR) to 0.94 (in the case of temperature-dependent TCR) at a thermal bias of only 5 K, just above absolute zero.

Except for the RhFe -  $\text{Al}_2\text{O}_3$  pair, literature data for TCR function near absolute zero are scarce, leaving the steepest region of the TCR function unresolved. Consequently, Figure 3b for the C - Au pair shows no improvement, or even a reduction, in RF values at the lowest temperatures. At slightly higher temperatures (10-20 K), however, the C - Au pair exhibits a moderate RF increase of up to 27 % (from 0.73 to 0.92 at  $T_{\text{cold ter.}} = 16$  K and  $\Delta T = 45$  K).

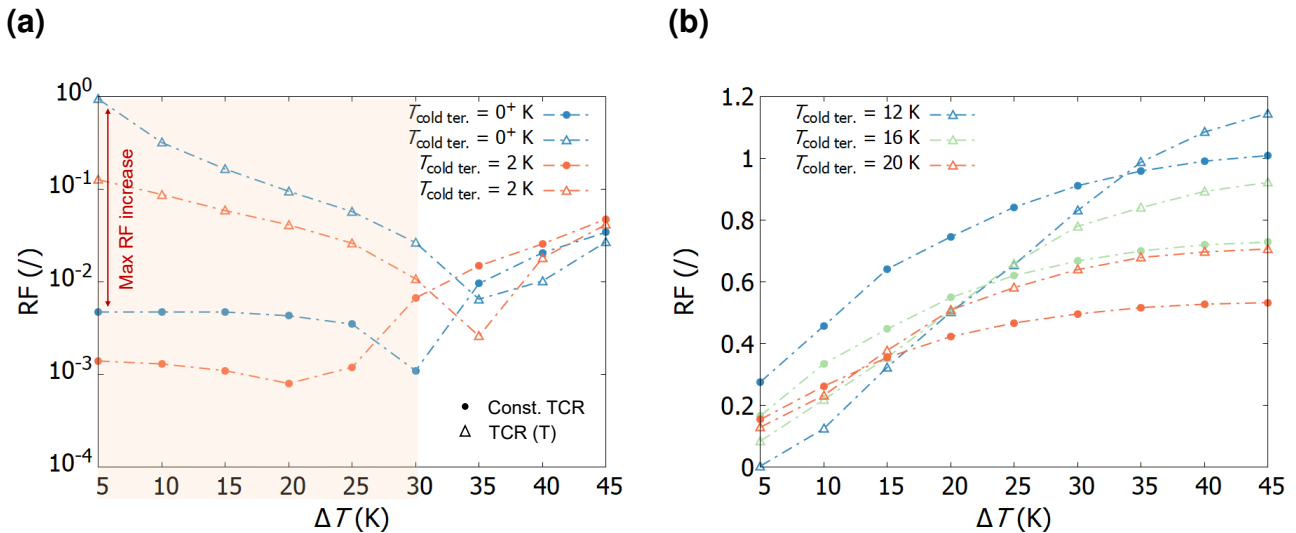


**Figure 3.** Influence of temperature-dependent TCR on RF for the selected MSTDs, plotted against  $\Delta T$ , at different cold terminal temperatures. The filled circles represent the values of RF at constant TCR, the empty triangles the RF values at temperature-dependent TCR. **(a)** RhFe -  $\text{Al}_2\text{O}_3$  pair, plotted on a logarithmic scale. **(b)** C - Au pair, plotted on a linear scale.

The present analysis of temperature-dependent TCR effects indicates that this factor can

be exploited to improve thermal rectification in cryogenic environments. Potential applications for cryogenic MSTDs include integration into the thermal management architecture of spacecraft<sup>[7]</sup>, cryogenic electronics<sup>[8]</sup>, and low-temperature sensor systems<sup>[9]</sup>. In these contexts, MSTDs can suppress parasitic heat loads and protect temperature-sensitive components. This work provides a foundation for future experimental validation and targeted design optimization of MSTDs. In particular, further exploration of the interplay between thermal conductivity and (temperature-dependent) TCR, along with the effects of thermal expansion, will be important.

## References

1. Klinar, K., Muñoz Rojo, M., Kutnjak, Z., and Kitanovski, A. (2020). Toward a solid-state thermal diode for room-temperature magnetocaloric energy conversion. *J. Appl. Phys.* *127*, 234101.
2. Zhao, H., Yang, X., Wang, C., Lu, R., Zhang, T., Chen, H., and Zheng, X. (2023). Progress in thermal rectification due to heat conduction in micro/nano solids. *Mater. Today Phys.* *30*, 100941.
3. Zhao, J., Wei, D., Gao, A., Dong, H., Bao, Y., Jiang, Y., and Liu, D. (2020). Thermal rectification enhancement of bi-segment thermal rectifier based on stress induced interface thermal contact resistance. *Appl. Therm. Eng.* *176*, 115410.
4. Dhuley, R.C. (2019). Pressed copper and gold-plated copper contacts at low temperatures - A review of thermal contact resistance. *Cryogenics* *101*, 111–124.
5. Stoner, R.J., and Maris, H.J. (1993). Kapitza conductance and heat flow between solids at temperatures from 50 to 300 K. *Phys. Rev. B* *48*, 16373–16387.
6. Swartz, E.T., and Pohl, R.O. (1987). Thermal resistance at interfaces. *Appl. Phys. Lett.* *51*, 2200–2202.
7. Kim, H., Cheung, K., Auyeung, R.C.Y., Wilson, D.E., Charipar, K.M., Piqué, A., and Charipar, N.A. (2019). VO<sub>2</sub>-based switchable radiator for spacecraft thermal control. *Sci. Rep.* *9*, 11329.
8. Conway Lamb, I.D., Colless, J.I., Hornibrook, J.M., Pauka, S.J., Waddy, S.J., Frechtling, M.K., and Reilly, D.J. (2016). An FPGA-based instrumentation platform for use at deep cryogenic temperatures. *Rev. Sci. Instrum.* *87*, 014701.
9. Homulle, H., and Charbon, E. (2017). Performance characterization of altera and Xilinx 28 nm FPGAs at cryogenic temperatures. In 2017 International Conference on Field Programmable Technology (ICFPT). pp. 25–31.